Acoustic plasmons in two- and three-component degenerate Fermi gases, with application to the gallium arsenide electron-hole plasma

1989 J. Phys.: Condens. Matter 1 1809

(http://iopscience.iop.org/0953-8984/1/10/003)

J. Phys.: Condens. Matter 1 (1989) 1809–1829. Printed in the UK

Acoustic plasmons in two- and three-component degenerate Fermi gases, with application to the gallium arsenide electron–hole plasma

B Bennacer and A A Cottey
School of Physics, University of East Anglia, Norwich NR4 7TJ, UK

Received 18 July 1988, in final form 8 September 1988

Abstract. Acoustic plasmons in a two-component degenerate Fermi gas are analysed, using the random-phase approximation dielectric function with exact analytic continuation into the lower half of the complex frequency plane. The acoustic plasmon spectrum, in reduced variables, depends on four parameters—the ratio of Thomas–Fermi screening wavevectors of the two plasmas, the ratio of Fermi velocities, and the densities of the two plasmas. The dependence of the spectrum on these parameters is surveyed. The first two of the above-mentioned parameters are the most important. Acoustic plasmons can exist even when the two plasmas have equal effective mass. The range of parameters giving weakly damped acoustic plasmons is described. The spectrum has an abrupt cut-off (maximum wavevector); this corresponds to the onset of Landau damping in both plasmas. The experimental results of Pinczuk, Shah and Wolff on acoustic plasmons in the GaAs electron–hole plasma are reanalysed. For this purpose the extension to a three-component plasma is made, since the light holes, although few in number, have a significant effect on the results. In this system the 'upper acoustic plasmon' does not exist, contrary to what is implicitly assumed by Pinczuk, Shah and Wolff in their analysis. The 'lower acoustic plasmon' does exist, and its phase velocity agrees, within the errors of theory and experiment, with their experimental result.

1. Introduction

This paper is principally about acoustic plasmons in semi-metals or semiconductors whose charge carriers may be modelled as a two-component degenerate Fermi gas (figure 1). A brief report on the theory and results for zero-wavevector plasma waves was given in Cottey (1985). The two components are labelled by $i\,(=1, 2)$, and component i has ν_i spherical pockets, all equivalent by symmetry, with Fermi wavevector k_{Fi}, Fermi velocity v_{Fi}, Fermi energy e_{Fi}, effective mass m_i^* and $e_{Fi} = \hbar^2 k_{Fi}^2/2m_i^*$. We label the two plasmas such that $v_{F2} < v_{F1}$.

The two-component plasma sustains two plasma modes, whose spectra are sketched qualitatively in figure 2. In the case of negligible damping the polarisations of the two plasmas have relative phase 0 (π) for the ordinary (acoustic) plasmon. The ordinary plasmon is often called the optic plasmon, but we avoid this term because the analogy with optic phonons (and indeed also between acoustic plasmons and acoustic phonons) is not as close as figure 2 suggests. Thus, when the parameters of the two plasmas become the same, so a one-component system is achieved, it is the acoustic plasmon that disappears.

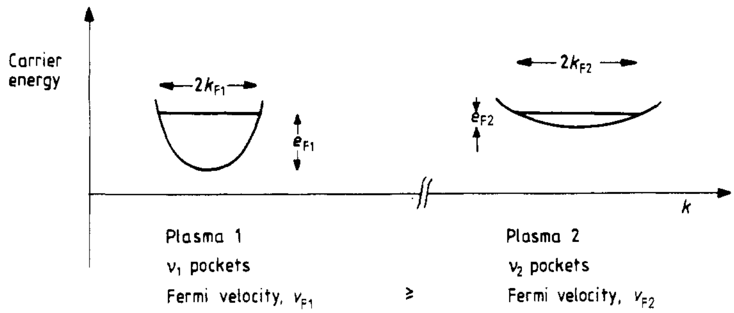

Figure 1. The model semi-metal. There are two kinds ($i = 1, 2$) of carrier.

The two types of carriers may be both electrons, or both holes, or one of each. The terms 'light' and 'heavy' to distinguish the two types of carrier, though commonly used in semiconductor physics, are not the best terms for our purpose, for, as we shall see, acoustic plasmons can exist when the two types have the same mass. What is essential for the existence of acoustic plasmons is that the two Fermi velocities be different.

We shall treat the ions in a jellium model, which nevertheless supplies a constant 'background' relative permittivity ε_{bg}. The value of ε_{bg} can be large, so the Coulomb interaction, $\sim e^2/\varepsilon_{bg}$, is much reduced. Then the high-density regime ($r_s^* \lesssim 1$) may be reached, even though the carrier density n is modest. The conditions under which a constant ε_{bg} may be used, and the appropriate value, will be discussed in § 5 and in another paper, on applications of the present theory.

Our analysis of acoustic plasmons is based on the frequency- (ω) and wavevector- (q) dependent longitudinal dielectric function $\varepsilon(q, \omega)$. The dispersion relations of the plasma modes are the solutions of

$$\varepsilon(q, \omega) = 0. \tag{1}$$

We consider a plasma wave with amplitude $\sim\exp[i(qx - \omega t)]$ with q real and positive, and $\omega = \omega' + i\omega''$ complex. A damped wave has $\omega'' < 0$.

We use the random-phase approximation (RPA) in order to have an explicit form for ε. This function is usually named after Lindhard (1954). It appears not to be generally recognised that Lindhard's form is valid only for $\omega'' > 0$ or $\omega = 0+$, nor that the general form had been found earlier by Silin (1952a).

The calculation of ε involves, for any plasma component, and for q in the x-direction as we are assuming, an integration with respect to k_x, the x-component of wavevector $\boldsymbol{k}$ of a charge carrier. The integrand (for each component) has a simple pole in the complex k_x-plane. Landau (1946) pointed out that the integration must be on a contour in the complex k_x-plane which passes below all poles of the integrand. For $\omega'' > 0$, the pole occurs in the upper half of the complex k_x-plane, and integration with respect to k_x along the real axis is valid. For $\omega'' < 0$, the path of integration must be deformed so as to pass below the pole. The pole then contributes a Cauchy term to the integral, and this term has the consequence that (1) has a solution with $\omega'' < 0$. This Landau damping was calculated explicitly by Landau for a classical (Maxwell–Boltzmann statistics) plasma.

The corresponding treatment for a one-component degenerate Fermi gas was made by Silin (1952a, 1955) and presentations of the results in English appeared by Klimontovich and Silin (1960, 1961). The results are in an obscure notation (with conventions not fully explicit) and there are minor errors of presentation which are also different in different papers. Nevertheless, the results are correct apart from these minor errors, and it is surprising that they have rarely been cited and apparently not taken further till 1985. Cottey (1985) includes (equations (1) and (2) therein) a condensed statement of the RPA dielectric function with Landau damping, but it also contains an error of presentation; the term $2\pi i$ in equation (2) therein should be multiplied by the factor $(1 - \zeta^2)$. In the present paper we give a full exposition of Silin's dielectric function and its implications for acoustic plasmons, including numerically calculated acoustic plasmon spectra for a representative set of system parameters.

Early works on acoustic plasmons in a degenerate two-component Fermi gas, or on the similar system of plasma-ion waves in a metal, are by Silin (1952b, 1955), Pines (1956), Pines (1963, pp 248–9) and Froehlich (1968). Those results are reviewed from the Lindhard dielectric function point of view by Platzman and Wolff (1973). In the case $k_{F1} = k_{F2}$ and pocket degeneracies ν_1 and ν_2 both equal to 1, the acoustic plasmon spectrum for small q and $v_{F2} \ll v_{F1}$ is $\omega = vq$ with constant complex phase velocity

$$v = v' + iv'' = (v_{F1}v_{F2}/3)^{1/2} - i\pi v_{F2}/12.$$

The derivations of this result, other than Silin's, are not entirely satisfying. The singular integral in ε leads to a logarithmic term, and its phase is chosen tacitly and on physical grounds. For example, assuming the ln function to have its principal phase (the normal convention in the absence of other indication) leads to internal inconsistency in the argument of Platzman and Wolff.

The difficulties are compounded when the restriction $v_{F2} \ll v_{F1}$ is lifted, even in the $q = 0$ limit. Thus Appel and Overhauser (1982) calculated the spectrum of acoustic plasmons of a two-component degenerate Fermi gas by solving coupled Boltzmann transport equations. They included an exchange–correlation term, and assumed q small. The exchange–correlation term makes a quantitative but not a qualitative difference. If it is omitted, direct comparison with earlier treatments, and with ours, is possible. The RPA dielectric function $\varepsilon(q, \omega)$ which we use gives, in the limit $q \to 0$, with ω/q constant. the same theory as that of Appel and Overhauser, *provided* $\omega > 0$ or $\omega = 0+$. Appel and Overhauser solved their transport equations numerically and found *three* acoustic plasma modes.

Oliva and Ashcroft (1984) pointed out that Appel and Overhauser's conclusions are incorrect and flow from an incorrect treatment of damping. Appel and Overhauser use a theory valid for $\omega'' > 0$ or $\omega = 0+$, and calculate the damping by a perturbative method. This approach is not reliable.

Schaefer and von Baltz (1987) have extended the analysis of the transport equations, including a phenomenological term describing impurity scattering. Other theoretical studies of acoustic plasmons are by Chakraborty (1984), Ganguly and Wood (1972), Oliva and Ashcroft (1982), Pashitskiĭ (1969), Rothward (1972), Sinha and Varma (1983) and Vignale and Singwi (1982, 1985).

Studies of modes analogous to acoustic plasmons in inhomogeneous (usually layered) media are by Blank and Gulyaev (1984), Das Sarma and Quinn (1982), Heitmann (1986), Lomtev and Bol'shinskii (1985), Olego *et al* (1982) and Takada (1977). Experimental evidence for acoustic plasmons is discussed in § 5, with reanalysis of the experimental results of Pinczuk *et al* (1981) on the GaAs electron–hole plasma.

Apart from the early works by Silin (1952b, 1955) and Klimintovich and Silin (1960, 1961), and the recent work by Cottey (1985), we know of no analyses of plasmon damping in a degenerate plasma based on a fully deductive treatment starting from the RPA dielectric function *with its exact analytic continuation into the lower half of the complex frequency plane.* We consider that this method is, however, the safest way to analyse

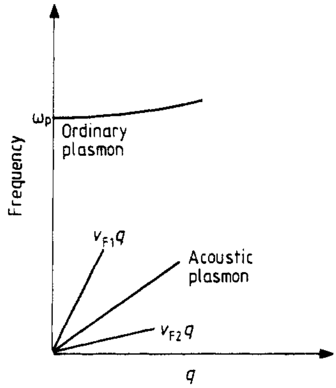

Figure 2. Sketch of the dispersion curves of the ordinary and acoustic plasmons in a two-component plasma.

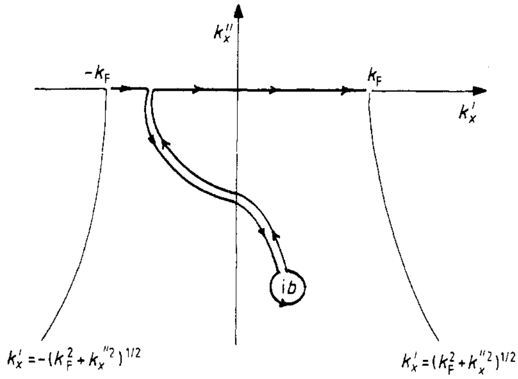

Figure 3. The contour in the complex k_x-plane of the singular integral involved in Silin's dielectric function $\varepsilon(q, \omega)$ with $\omega'' < 0$ (damped oscillation).

acoustic plasmons. It is exactly consistent with the principle of causality. Its limitations are solely those of the RPA.

In the following sections we present a derivation and discussion of the RPA dielectric function, in the lower half of the complex frequency plane, of a degenerate Fermi gas. This is done first for a one-component and then for a two-component Fermi gas. The limits of validity of the RPA are discussed. Then the plasmon dispersion curves—the solutions of (1)—are presented. After the extension of the theory from two to three components, the results are applied to the gallium arsenide electron–hole plasma. The paper ends with a general discussion of the range of phenomena that may be expected for system parameters achievable in real semi-metals and semiconductors.

2. The model

The plasma model was defined in § 1 (see also figure 1). We define the dielectric function $\varepsilon(q, \omega)$ as (permittivity of system)/$\varepsilon_0\varepsilon_{bg}$ where ε_0 is the permittivity of vacuum. The dielectric function ε is related to the polarisation function $\chi(q, \omega)$ of the carrier gas by

$$\varepsilon = 1 - e^2\chi/\varepsilon_0\varepsilon_{bg}q^2 \qquad \text{(SI units)}.$$

In the RPA, χ is given by

$$\chi(q, \omega) = \frac{2}{(2\pi)^3}\int \mathrm{d}^3k \frac{n(\boldsymbol{k}) - n(\boldsymbol{k}+\boldsymbol{q})}{\hbar(\omega - \omega_{k,q})} \tag{2}$$

where $n(\boldsymbol{k})$ is the Fermi–Dirac occupation probability of a carrier state with wavevector $\boldsymbol{k}$,

$$\hbar\omega_{k,q} = e_{k+q} - e_k = \hbar^2(q^2 + 2\boldsymbol{q}\cdot\boldsymbol{k})/2m^*$$

is the change of carrier energy upon the transition $\boldsymbol{k} \to \boldsymbol{k} + \boldsymbol{q}$ and $\omega'' > 0$ or $\omega'' = 0+$.

We assume the carrier pockets separated in $\boldsymbol{k}$-space by wavevectors large compared with k_{F1} and k_{F2} and the largest q of interest. Then, since the gases are assumed degenerate, only intra-pocket transitions occur, and the integral in (2) has ν_1 equal contributions from plasma 1 and ν_2 equal contributions from plasma 2. Each of these contributions depends only on q $(= |\boldsymbol{q}|)$.

3. One-component plasma

In this section we drop the component label i.

3.1. Dielectric function

Considering a given pocket, we take the origin of $\boldsymbol{k}$ at the centre of the pocket. The analytic continuation is clearer if we keep the temperature T finite at this stage, so

$$n(\boldsymbol{k}) = \{1 + \exp[(k_x^2 + k_\rho^2 - k_\mathrm{F}^2)/k_T^2]\}^{-1}$$

where k_ρ is the magnitude of the projection of $\boldsymbol{k}$ into the plane normal to $\boldsymbol{q}$ and $k_T^2 = 2m^* k_\mathrm{B} T/\hbar^2$. Here k_ρ is real, but when $\omega'' < 0$, k_x may be complex.

The first, $n(\boldsymbol{k})$, of the two n-terms in equation (2) gives, after the k_ρ integration has been done,

$$\frac{-m^*}{h^2 q} \int_{-\infty}^{\infty} \frac{\mathrm{d}k_x}{k_x - \mathrm{i}b} k_T^2 \ln\{1 + \exp[(k_\mathrm{F}^2 - k_x^2)/k_T^2]\}$$

where

$$b = (-\mathrm{i}m^*/\hbar q)(\omega - \hbar q^2/2m^*).$$

This holds for any fixed complex k_x, and in the limit $T \rightarrow 0$ is

$$\frac{-m^*}{h^2 q} \int_{-\infty}^{\infty} \frac{\mathrm{d}k_x}{k_x - \mathrm{i}b} (k_\mathrm{F}^2 - k_x^2)\theta(k_\mathrm{F}^2 - \mathrm{Re}(k_x^2)). \tag{3}$$

Dealing first with the case $\omega'' > 0$, we note that the k_x integration is then from $-k_\mathrm{F}$ to k_F on the real line. It is convenient to express ε as a function of

(i) the reduced wavevector $z = q/2k_\mathrm{F}$ and
(ii) the reduced phase velocity $u = \omega/qv_\mathrm{F}$ instead of q and ω. The integral in (3) is

$$k_\mathrm{F}^2[2(z-u) + \mathscr{F}_+(z-u)]$$

where

$$\mathscr{F}_+(\zeta) = (1 - \zeta^2)\ln[(\zeta+1)/(\zeta-1)]. \tag{4}$$

Throughout this paper the ln function has its principal phase, i.e. $-\pi <$ phase $\leqslant \pi$.

Calculating the $n(\boldsymbol{k}+\boldsymbol{q})$ term in (2) in like manner, and summing over ν pockets, we find for a one-component plasma

$$\varepsilon(z,u) = 1 + (\kappa_\mathrm{TF}/k_\mathrm{F})^2 g_+(z,u) \qquad (u'' > 0 \text{ or } u'' = 0+)$$

where

$$g_+(z,u) = (2z)^{-2}\{\tfrac{1}{2} + (8z)^{-1}[\mathscr{F}_+(z-u) - \mathscr{F}_+(-z-u)]\} \qquad (u''>0 \text{ or } u''=0+) \tag{5}$$

$$\kappa_\mathrm{TF} = 3^{1/2}\omega_\mathrm{p}/v_\mathrm{F} \qquad \omega_\mathrm{p} = (ne^2/m^*\varepsilon_0\varepsilon_\mathrm{bg})^{1/2}$$

and $n = \nu k_\mathrm{F}^3/3\pi^2$ is the carrier density. The property

$$\varepsilon(0,\omega) = 1 - (\omega_\mathrm{p}/\omega)^2$$

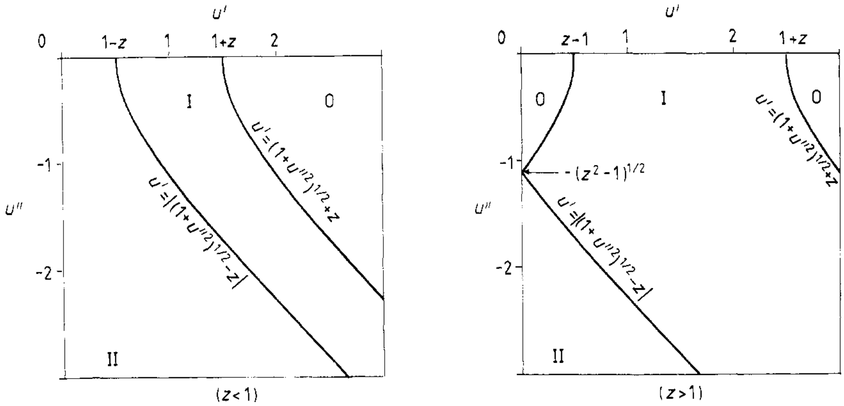

Figure 4. For a fixed z, we define three regions in the complex u-plane which help us survey the properties of the dielectric function $\varepsilon(z, u)$. In region 0, both 'extra terms' $\Delta\mathscr{F}$ are zero. In region I, $\Delta\mathscr{F}(z-u)$ is non-zero but $\Delta\mathscr{F}(-z-u)$ is zero. In region II, both $\Delta\mathscr{F}$ terms are non-zero.

shows that ω_p is the usual plasma frequency parameter, and the property

$$\varepsilon(q, 0) \sim (\kappa_{\mathrm{TF}}/q)^2 + \mathrm{O}(1) \qquad q \to 0$$

shows that κ_{TF} is the usual Thomas–Fermi screening wavevector.

If $\omega'' < 0$ (damped oscillation) the contour of the k_x integration (3) is deformed to pass below the pole at $k_x = ib$ (figure 3). If this pole lies in the region where the Fermi–Dirac function has the value 1, i.e. $\mathrm{Re}(k_x^2) < k_F^2$, its effect is to add $2\pi\mathrm{i}$ to the ln in (4), i.e. $2\pi\mathrm{i}(1-\zeta^2)$ is added to $\mathscr{F}_+$. Thus the general expression for the dielectric function of a one-component degenerate Fermi gas with ν spherical pockets having a parabolic energy–wavevector relation is

$$\varepsilon(z, u) = 1 + (\kappa_{\mathrm{TF}}/k_F)^2 g(z, u) \qquad (6)$$

where g is the same as g_+ (equation (5)) except that $\mathscr{F}_+$ is replaced by

$$\mathscr{F} = \mathscr{F}_+ + \Delta\mathscr{F}$$

where

$$\Delta\mathscr{F}(\zeta) = \begin{cases} 2\pi\mathrm{i}(1-\zeta^2) & \zeta'' > 0 \text{ and } \zeta'^2 < 1 + \zeta''^2 \\ 0 & \text{otherwise} \end{cases}$$

$$\zeta = \zeta' + \mathrm{i}\zeta''.$$

The function ε' ($\varepsilon = \varepsilon' + \mathrm{i}\varepsilon''$) is discontinuous on the lines

$$u' = |(1 + u''^2)^{1/2} \pm z| \qquad (7)$$

but ε'' is continuous. These discontinuities are consequences of the discontinuity of the Fermi–Dirac function. We find it convenient to define three regions (figure 4) of complex u-space (with z fixed). The lines (7) separate distinct regions.

If the damping u'' is zero, equations (7) become

$$u' = |1 \pm z|.$$

The functions $|1 \pm z|$ are plotted in figure 5, together with their more conventional representation as ω versus q. The lines $1 + z$ and $z - 1$ ($z \geqslant 1$) are boundaries of the

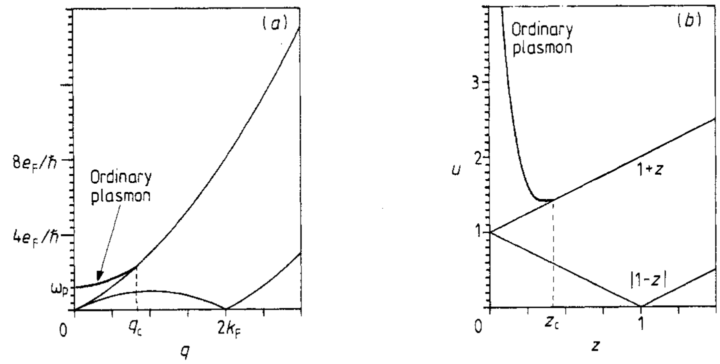

Figure 5. The lines of discontinuity, relating to the electron–hole pair continuum, in a one-component plasma without damping. (*a*) Frequency ω versus wavevector q. (*b*) reduced phase velocity $u = \omega/qv_F$ versus reduced wavevector $z = q/2k_F$.

particle–hole pair continuum. The line $1 - z$ $(0 \leqslant z \leqslant 1)$ also has a special significance in connection with the density of states $\mathscr{D}(\omega)$ of particle–hole excitations: $d\mathscr{D}/d\omega$ is discontinuous on this line.

3.2. *Range of validity of the* RPA

A precise characterisation of the accuracy of the RPA is not known. We shall follow the usual approximate criteria for validity of the RPA (Platzman and Wolff 1973). The RPA is a high-density theory, and the criterion for sufficiently high density is, for a one-component single-pocket plasma,

$$r_s^* \lesssim 1 \tag{8}$$

where

$$a_B^* r_s^* = R_s = (3/4\pi n)^{1/3}$$

and

$$a_B^* = 4\pi\varepsilon_0\varepsilon_{bg}\hbar^2/e^2m^*.$$

Condition (8) comes from the condition

$$\frac{\text{mean KE per particle}}{\text{characteristic PE per particle}} = (3\hbar^2k_F^2/10m^*)/(e^2/4\pi\varepsilon_0\varepsilon_{bg}R_s) \gtrsim \tfrac{3}{10}(9\pi/4)^{2/3}. \tag{9}$$

If the KE/PE ratio is not sufficiently large, the charge carriers will take up a more complex correlation than that given by the simple screening in the RPA.

The RPA is also inaccurate for waves with too large wavevector (Platzman and Wolff 1973), and we take the usual validity condition

$$q \lesssim q_{max} = \omega_p/v_F = 3^{-1/2}\kappa_{TF}. \tag{10}$$

In the case of ν pockets we shall write r_{ssp}^* for the single pocket reduced density parameter, defined by

$$(4\pi/3)(r_{ssp}^* a_B^*)^3 = \nu/n$$

n being the carrier density with all pockets counted.

Parameters κ_{TF}, k_F and r_{ssp}^* are related by

$$(\kappa_{TF}/k_F)^2 = (4/\pi)(4/9\pi)^{1/3}\nu r_{ssp}^* = 2c\nu \tag{11}$$

where c is introduced as a convenient shortened notation, and

$$c \simeq r^*_{\mathrm{ssp}}/3$$

to a close approximation.

Equation (10) may be rewritten in the forms

$$z \leqslant z_{\max} = q_{\max}/2k_{\mathrm{F}} = (c\nu/6)^{1/2} \simeq (r^*_{\mathrm{ssp}}\nu/18)^{1/2}. \tag{12}$$

3.3. Ordinary plasmon

For completeness we state briefly the results in the one-component case. Equation (1) gives but one dispersion curve. (Oliva and Ashcroft (1984) showed that the application of Appel and Overhauser's (1982) method to a one-component plasma gives, erroneously, two solutions.) At small wavevector, $\omega = \omega_{\mathrm{p}}$ and is in region 0 (figure 4). There is no damping until wavevector $q_{\mathrm{c}} = 2k_{\mathrm{F}}z_{\mathrm{c}}$ is reached, at which, according to this RPA theory, the plasma dispersion branch meets the line $1 + z$ (figure 5(*b*)). The critical value z_{c} is usually near to, or greater than, $z_{\max}$ (defined in equation (12)).

4. Two-component plasma

4.1. Dielectric function

We restore the component index i $(= 1, 2)$ and choose 2 as the reference plasma, i.e. the reduced wavevector and phase velocity are now defined by

$$z = q/2k_{\mathrm{F2}} \qquad u = \omega/qv_{\mathrm{F2}}.$$

We also write r_v for v_{F2}/v_{F1} and r_k for $k_{\mathrm{F2}}/k_{\mathrm{F1}}$.

Then, from (6) and (11), the dielectric function of the two-component plasma, allowing only for intra-pocket transitions as explained in § 2, is

$$\varepsilon(z, u) = 1 + 2c_1\nu_1 g(r_k z, r_v u) + 2c_2\nu_2 g(z, u)$$

where

$$c_i = (2/\pi)(4/9\pi)^{1/3} r^*_{\mathrm{ssp}i} \simeq \tfrac{1}{3}r^*_{\mathrm{ssp}i} \qquad (i = 1, 2)$$

are convenient density parameters.

The dielectric function, in terms of the reduced wavevector and phase velocity, depends on the four parameters $c_2\nu_2$, $c_1\nu_1$, r_k and r_v.

4.2. Discontinuities

Now ε' has, in addition to the lines of discontinuity (7) associated with plasma 2, the lines of discontinuity

$$u' = |(r_v^{-2} + u''^2)^{1/2} \pm r_k z/r_v| \tag{13}$$

associated with plasma 1. These lines are sketched in u'–u'' space (with z fixed) in figure 6.

We shall also find it convenient to compare $u'(z)$ with the functions

$$d_{2\pm}(z) = |(1 + u''(z)^2)^{1/2} \pm z| \tag{14}$$

and

$$d_{1\pm}(z) = |[r_v^{-2} + u''(z)^2]^{1/2} \pm r_k z/r_v| \tag{15}$$

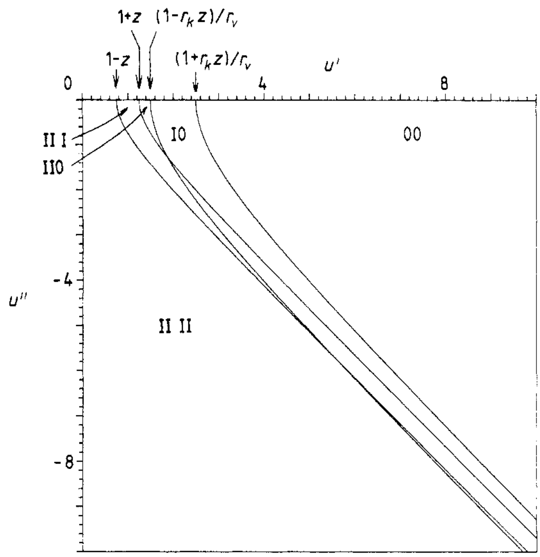

Figure 6. The lines of discontinuity of ε' in the complex u-plane for fixed z. This figure is for the case $z < 1$ and $z < (1 - r_v)/(r_v + r_k)$. Several other qualitatively distinct cases give obvious modifications of this diagram. Region II0, for example, means region II for plasma 1 and region 0 for plasma 2.

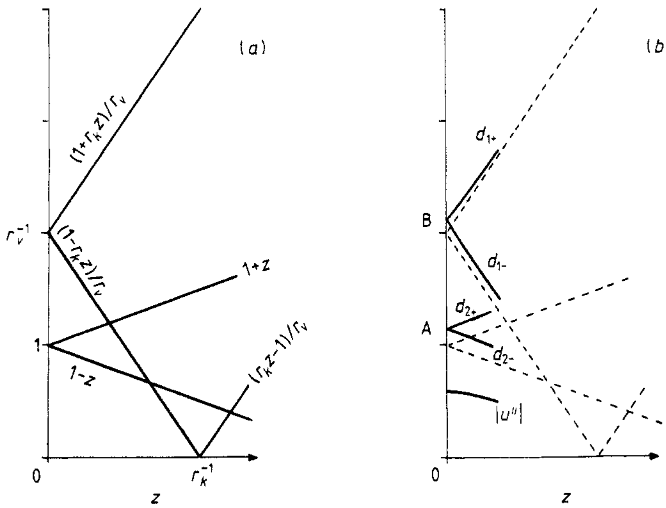

Figure 7. (a) The lines of discontinuity $|1 + z|$ and $|1 \pm r_k z|/r_v$ for a two-component plasma with damping neglected; $z = \text{wavevector}/2k_{F2}$. ($b$) Sketch (for small z) of the corresponding functions, namely $d_{2\pm}$, $d_{1\pm}$ (equations (14) and (15)) when damping u'' is included.

in a diagram (figure 7(b)). The special case $u'' = 0$, when the d-functions become $|1 \pm z|$ and $|1 \pm r_k z|/r_v$ is represented in figure 7(a), which is the generalisation to the two-component case of figure 5(b).

4.3. *Plasmons at zero wavevector*

The limit $z \to 0$ of $\varepsilon(z, u)$ may be taken in two ways, which give distinct plasma solutions of $\varepsilon = 0$. If we keep ω constant and non-zero, i.e. take lim $z \to 0$ with $uz = \text{constant} > 0$, then ε becomes

$$1 - (\omega_{p1}^2 + \omega_{p2}^2)/\omega^2 \qquad (\omega_{pi}^2 = n_i e^2/\varepsilon_0 \varepsilon_{bg} m_i^*)$$

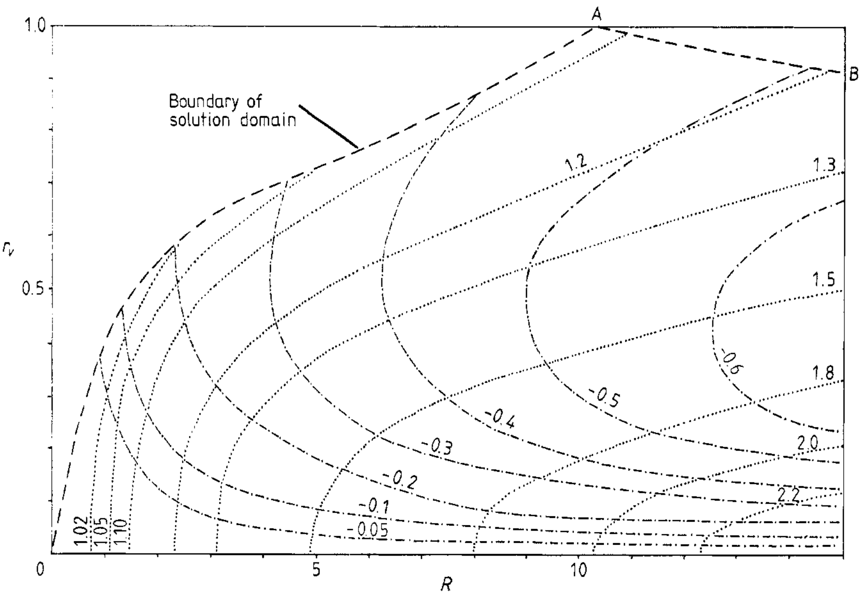

Figure 8. Contours of u' (· · · ·) and u'' (—·—·—) for zero wavevector in the space of the parameters R $(=(\kappa_{\mathrm{TF2}}/\kappa_{\mathrm{TF1}})^2)$ and r_v $(=v_{\mathrm{F2}}/v_{\mathrm{F1}})$. Here $u = u' + \mathrm{i}u''$ is the reduced complex phase velocity of acoustic plasmons.

and $\varepsilon = 0$ has the ordinary plasmon solution with frequency $(\omega_{\mathrm{p1}}^2 + \omega_{\mathrm{p2}}^2)^{1/2}$. The generalisation to a two-component plasma introduces no remarkable new features, either at $z = 0$ or for $z > 0$, and we will not discuss the ordinary plasmon further.

If $\lim z \to 0$ is taken with $u =$ constant (case of acoustic plasmon) the equation $\varepsilon = 0$ becomes

$$F(r_v u) + RF(u) = 0 \tag{16}$$

where

$$F(u) = 1 + \tfrac{1}{2}u \ln[(u-1)/(u+1)] + \begin{cases} \mathrm{i}\pi u & u'' < 0 \text{ and } u'^2 < 1 + u''^2 \\ 0 & \text{otherwise} \end{cases}$$

and

$$R = (\kappa_{\mathrm{TF2}}/\kappa_{\mathrm{TF1}})^2 = r_k^2 c_2 \nu_2 / c_1 \nu_1 = r_k^2 \nu_2 / r_v \nu_1 .$$

Only two parameters, r_v and R, are needed to describe all zero-wavevector cases. The results of numerical solution of (16) for all r_v (which is by definition $\leqslant 1$) and for $R \leqslant 15$ are shown in figure 8. (A small error in the contour $u'' = -0.5$ in figure 1 of Cottey (1985) is here corrected.) The existence of the abrupt edges of the solution domain relates to discontinuities of ε': line 0A is given by the relation

$$u' = (1 + u''^2)^{1/2}$$

which is the $z = 0$ limit of equations (7). Line AB is given by the relation

$$u' = (r_v^{-2} + u''^2)^{1/2}$$

which is the $z = 0$ limit of equations (13).

When

$$Rr_v^2 \ll 1 \ll R^2 \tag{17}$$

equation (16) may be solved analytically, the result being

$$u' = (R/3)^{1/2} \qquad u'' = -\pi R r_v/12. \tag{18}$$

This is essentially the special case in terms of which acoustic plasmons are usually discussed (for example, Silin 1952b, 1955, Pines 1963, Froehlich 1968, Platzman and Wolff 1973, Ruvalds 1981). Most of the discussions of acoustic plasmons are subject also to the further restrictions

$$\nu_1 = \nu_2 = 1 \qquad \text{and} \qquad n_1 = n_2 \qquad (\text{whence } k_{F2} = k_{F1}). \tag{19}$$

Then both of the inequalities (17) and the condition for relatively small damping

$$|u''|/u' \ll 1$$

all amount to

$$m_1^* \ll m_2^*.$$

More generally, this condition is not necessary. Weakly damped acoustic plasmons can even exist with $m_1^* = m_2^*$. For example, a system with $r_k = r_v = 0.25$ and $\nu_2/\nu_1 = 4$ has $R = 1$, and at zero wavevector $u' = 1.03$, $u'' = -0.039$. Indeed, the damping is always small in the lower left corner of figure 8. In this region (say $R \lesssim 1$, $r_v \lesssim 0.4R$) there is an approximate analytic solution, namely

$$u = 1 + \delta u$$

with

$$\delta u = 2[(1 + r_v)/(1 - r_v)]^{r_v/R} \exp[-2(1 + R^{-1})] \exp(-\mathrm{i}\pi r_v/R).$$

Since the damping is exponentially small, we should however expect to reach easily a regime in which the dominant damping mechanisms are beyond the RPA (collisions, or multi-particle processes).

4.4. *Acoustic plasmons at finite wavevector*

4.4.1. Validity of RPA. In the two-component plasma we use, as an approximate density condition, the criterion (9) with $R_s = (3/4\pi n)^{1/3}$. Here $n = n_1 + n_2$ is the total carrier density for both plasmas. This condition leads to

$$c_1 \nu_1^{1/3} \lesssim \tfrac{1}{3}(1 + R r_e^2)/(1 + R r_e)^{4/3}$$

where

$$r_e = r_k r_v = e_{F2}/e_{F1}.$$

In acoustic plasmons the polarisations of the two plasmas partially cancel each other. For this reason an appropriate wavevector criterion for the validity of the RPA is that (12) should apply for each component separately:

$$z_{\max} = \min\{(c_2 \nu_2/6)^{1/2}, r_k^{-1}(c_1 \nu_1/6)^{1/2}\}.$$

A number of theories of the electron gas incorporating corrections to the RPA and giving an improved description at large wavevector have been proposed; see Singwi and Tosi (1981) for a review. The exact analytic continuation of the dielectric functions of these theories into the lower half of the complex frequency plane appears to be a more difficult task, so we have limited our analysis to wavevectors and densities for which the

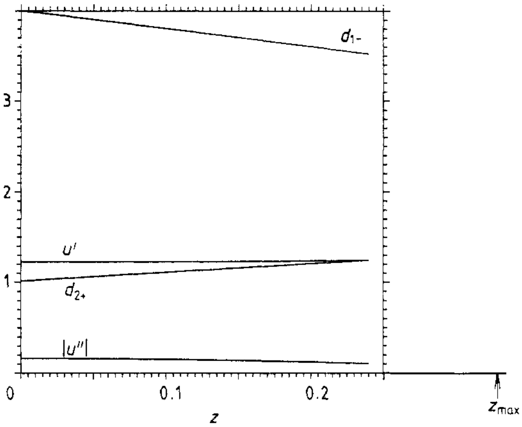

Figure 9. Acoustic plasmon spectrum for system B3. u' = Re(acoustic plasmon phase velocity)/v_{F2}. u'' is the corresponding imaginary part, and is a measure of damping. z = wavevector/$2k_{F2}$. The d-functions are defined in equations (14) and (15). For B3, $c_2\nu_2 = 1.92$, $c_1\nu_1 = 0.16$, $r_k = 0.5$, $r_v = 0.25$ and $R = 3$.

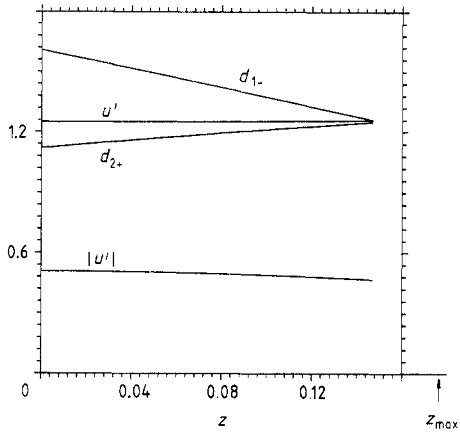

Figure 10. An example of a system (B12) whose acoustic plasmon ends when the lines d_{1-} and d_{2+} are close together. For B12, $c_2\nu_2 = 1.92$, $c_1\nu_1 = 0.42$, $r_k = 1.5$, $r_v = 0.6554$ and $R = 10.3$.

RPA is approximately valid.

4.4.2. Acoustic plasmon spectra. In this section we present numerically calculated spectra (u' and u'' versus z) of acoustic plasmons for several sets of the four parameters $c_2\nu_2$, $c_1\nu_1$, r_k and r_v that characterise our model. These results provide an overview of the possibilities for semi-metals and degenerate semiconductors. Calculations for specific substances will be presented in § 5 and in another paper.

The task of surveying the possibilities in the four-parameter family of systems is simplified by the fact that the zero-wavevector results, $u'(0)$ and $u''(0)$, depend only on two parameters, r_v and R, and these results were analysed fully in § 4.3.

We find numerically that, when an acoustic plasmon exists at all, it exists at zero wavevector and the inequality

$$[1 + u''(0)^2]^{1/2} < u' < [r_v^{-2} + u''(0)^2]^{1/2}$$

is satisfied. That is, the spectrum $u'(z)$ always starts with $u'(0)$ somewhere on the interval AB in figure 7(b). The acoustic plasmon at zero wavevector is Landau-damped by plasma 1 but not by plasma 2.

Turning now to $z > 0$, we may expect the spectrum $u'(z)$ to be continuous until it meets one of the lines $d_{2+}(z)$, $d_{1-}(z)$. Then ε' is discontinuous, and we may anticipate either a jump of the acoustic plasmon spectrum, or its disappearance. These expectations are borne out by numerical calculation. The first critical wavevector, at which the first segment of the acoustic plasmon spectrum ends, will be written $q_{c1} = 2k_{F2}z_{c1}$. This first segment is in the region of figure 6 designated II0. Bennacer (1987) has shown analytically that a small-z solution does not exist in region II II.

We start the presentation of numerical results with system B3 ($c_2\nu_2 = 1.92$, $c_1\nu_1 = 0.16$, $r_k = 0.5$, $r_v = 0.25$; these parameters imply $R = 3$, $\nu_2/v_1 = 3$ and $m_2^*/m_1^* = 2$). The acoustic plasmon spectrum is shown in figure 9. This system's coordinates in figure 8 ($R = 3$, $r_v = 0.25$) make it nearer to the boundary 0A (on which $u' = (1 + u''^2)^{1/2}$) than to the boundary AB (on which $u' = (r_v^{-2} + u''^2)^{1/2}$). We therefore expect that, as z increases above zero, u' will meet the line of discontinuity $d_{2+}(z)$

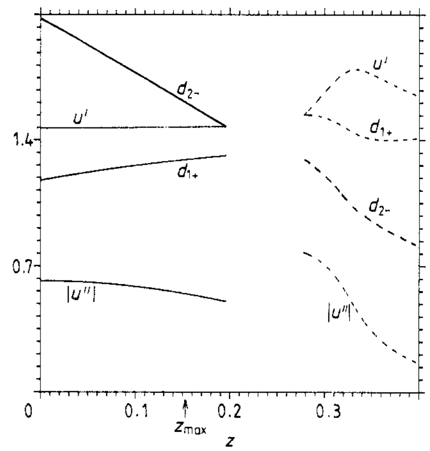

Figure 11. Graph for system B11 including part of the second segment (broken curves). See text for discussion. For B11, $c_2\nu_2 = 1.92$, $c_1\nu_1 = 0.32$, $r_k = 1.5$, $r_v = 0.5$ and $R = 13.5$.

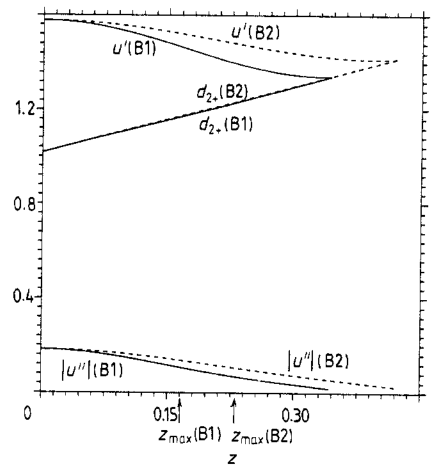

Figure 12. The acoustic plasmon spectrum (systems B1 and B2), apart from its cut-off, varies only weakly if the density of both plasma components is scaled by the same factor. For B1, $c_2\nu_2 = 0.984$, $c_1\nu_1 = 0.041$; for B2, $c_2\nu_2 = 1.92$, $c_1\nu_1 = 0.08$; for both, $r_k = 0.5$, $r_v = 0.125$ and $R = 6$.

in figure 9, and this is found numerically to be the case.

Other features of the results (figure 9) for system B3, which we have found to hold for all the systems we have studied, are

(i) u' and u'' vary only slowly with z (within the range of validity of the RPA); and
(ii) both u' and u'' have the form $a + bz^2$ for small z; in the case of u'', $b > 0$ always; further, $|u''|$ is a decreasing function of z throughout the range $0 < z \leqslant z_{c1}$.

If $R \leqslant 9$, the results are qualitatively similar to those of the system just discussed, as may be anticipated from figure 8. In some other systems, the acoustic plasmon spectrum $u'(z)$ meets the line d_{1-}, instead of the line d_{2+}.

Figure 10 shows an example (system B12) for which u' meets d_{1-}, but d_{2+} is near. This has no startling effect on the first segment of the spectrum. Another feature of system B12 is that acoustic plasmons occur up to reasonably large wavevectors, even though r_v is not much less than unity. The damping is, however, rather strong.

Many of the systems studied have second, and sometimes even more, segments at large z. Figure 11 includes the beginning of the second segment for system B11. We tried to find system parameters for which the second segment started at a wavevector $z_{c2} < z_{max}$, but although we identified the optimal parameters for this, we found no such systems, and indeed no system with z_{c2} near z_{max}. We conclude that a valid second segment might conceivably exist in some real systems, but the RPA indications are negative.

In the first two examples given so far (figures 9 and 10) the spectrum comes to an abrupt end at a wavevector z_{c1} that is less than z_{max}. Thus the sharp cut-off of the acoustic plasmon spectrum is for these systems a definite prediction of the theory. In other systems, for example B11 (figure 11), the first segment is qualitatively similar to those discussed earlier, but $z_{max} < z_{c1}$.

Figure 12 compares two systems which differ only by a common scaling of density

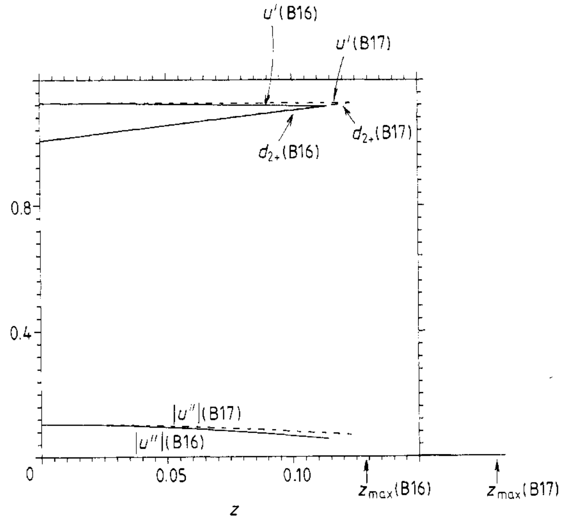

Figure 13. Investigation of the dependence of the acoustic plasmon spectrum (systems B16 and B17) on the ratio ν_2/ν_1 of pocket numbers. $R = 2$, $r_v = 0.25$ and $c_2\nu_2c_1\nu_1 = 0.02$ are the same for the two systems; for B16, $c_2\nu_2 = 0.2$, $c_1\nu_1 = 0.1$; for B17, $c_2\nu_2 = 0.4$, $c_1\nu_1 = 0.05$. Since $c_1/\nu_1 = r_v$, $\nu_2\nu_1$ is determined. It is 0.5 for system B16 and 2 for system B17.

of both plasma components. The features of the reduced spectrum, other than the cut-off z_c, depend weakly on such a scaling.

The acoustic plasmon spectrum also depends only weakly on the ratio ν_2/ν_1 of pocket numbers if R, r_v and $c_2\nu_2c_1\nu_1$ are held constant. This is illustrated in figure 13.

Numerical results for other values of the parameters are presented in Bennacer (1987).

4.5. *Summary of properties of acoustic plasmon spectra*

(i) The reduced complex phase velocity $u(=$ complex phase velocity$/v_{F2})$ of acoustic plasmons as a function of the reduced wavevector z $(=$ wavevector$/2k_{F2})$ depends on four parameters of our model, $c_2\nu_2$, $c_1\nu_1$, r_v and R, where $\nu_i =$ number of pockets in plasma i $(i = 1, 2)$ $c_i = (2/\pi)(4/9\pi)^{1/3}r^*_{sspi}$ with r^*_{sspi} the usual r_s density parameter for a single pocket of plasma i, $r_v = v_{F2}/v_{F1}$, and $R = (\kappa_{TF2}/\kappa_{TF1})^2$ with κ_{TFi} the Thomas–Fermi screening wavevector of plasma i.

(ii) At zero wavevector u depends only on the two parameters, r_v and R. Figure 8 shows the domain of these parameters for which acoustic plasmons exist, and shows also contours of constant u' and constant u'' within this domain.

(iii) When acoustic plasmons exist in a system, the theory predicts a branch $0 \leqslant z \leqslant z_{c1}$ of the spectrum, with a sharp cut-off at z_{c1}. In this branch, u' is usually approximately constant, and $|u''|$ decreases with increasing z. Sometimes z_{c1} is less and sometimes greater than the limit z_{max} of validity of the RPA.

(iv) The theory often produces further segments of the acoustic plasmon spectrum at larger z, but no part of such a segment has even been found with $z < z_{max}$.

(v) Determining $u'(0)$ and $u''(0)$ from figure 8, and sketching $u' \simeq$ constant until the first discontinuity in figure 7(b) is reached, or to $z = z_{max}$ if that is less, is a simple procedure which usually predicts the acoustic plasmon spectrum to a useful degree of accuracy. Of the four parameters of the full model, the two parameters r_v and R determining the properties at zero wavevector are the most important.

(vi) The damping of acoustic plasmons is small in the lower left portion of figure 8, and remains small for all wavevectors up to the sharp cut-off or the RPA limit.

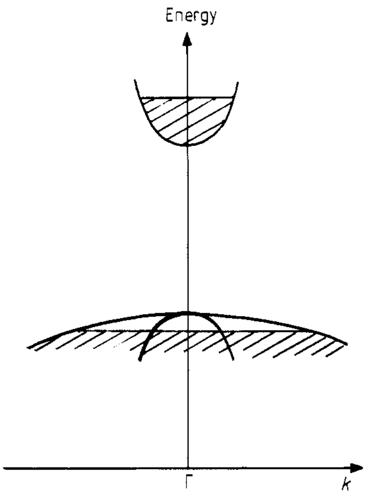

Figure 14. The GaAs electron–hole plasma.

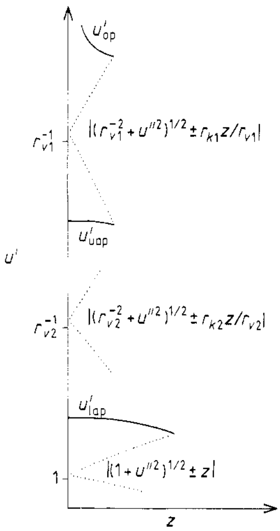

Figure 15. Qualitative sketch of the dispersion curves, real part (u') of reduced phase velocity versus reduced wavevector z of plasma modes in a three-component plasma. The first segment of a dispersion curve ends when it meets one of the lines of discontinuity (······). Subscripts: op = ordinary plasmon, uap = upper acoustic plasmon, lap = lower acoustic plasmon.

5. Extension to three components and application to the GaAs electron–hole plasma

The photo-excited electron–hole plasma (figure 14) in GaAs studied by Pinczuk *et al* (1981) (PSW) consists of equal densities of electrons and holes: $n_e = n_{lh} + n_{hh}$, where lh and hh stand for light and heavy holes. The electrons come rapidly to equilibrium with each other and form a degenerate electron gas. Likewise the holes form a degenerate hole gas. Spectroscopy to measure acoustic plasmons (or other properties of the electron–hole plasma) is done within the time that the electrons take to relax by 'forbidden' transitions to the valence band.

It is necessary to treat this system as a *three-component* plasma, for although the light holes comprise only 4% of all holes, their neglect perturbs the final result (acoustic plasmon velocity) by about 20%. The generalisation of the two-component theory given in the preceding sections is therefore presented. The theory assumes that the polarisation function of the plasma is the sum of contributions from each component separately. This is true if inter-pocket transitions are negligible, which is the case when the pockets are separated in k-space by wavevectors (usually ~ reciprocal-lattice vector) larger than the wavevector q of the plasma mode being considered, or are separated in energy by an amount greater than $\hbar\omega$, where ω is the frequency of the plasma mode. Neither of these conditions applies to the lh–hh pair of pockets. However, allowance for the Bloch nature of the states implies that the polarisation function for lh–hh transitions contains a factor beyond the effective-mass approximation used in the preceding sections, namely the square of the overlap integral of the Bloch u-functions (Wooten 1972). In the approximation of small q ($\ll$ reciprocal lattice vectors) this integral is

$$\langle k, \mathrm{lh} | k, \mathrm{hh} \rangle = \delta_{\mathrm{lh,hh}}$$

Table 1. Parameters of the GaAs systems and acoustic plasmon results. For both systems $r_{k2} = 2.88$, $r_{k1} = 0.986$, $r_{v2} = 0.348$, $r_{v1} = 0.108$ and the RPA density condition is $c_3 \leqslant 1.4$.

$n_e(10^{17}\ \mathrm{cm}^{-3})$		3	7
c_3		2.83	2.13
c_2		0.984	0.742
c_1		0.306	0.231
RPA wavevector condition: $z \leqslant$		0.14	0.11
z corresponding to $q = 74\ \mu\mathrm{m}^{-1}$		0.179	0.135
Acoustic plasmon energy (meV)	PSW calc.	3.4	4.6
	PSW expt	'in agreement'	
	Present calc., with $q = 74\ \mu\mathrm{m}^{-1}$	3.0	3.9
Damping: $\lvert\omega''/\omega'\rvert$ (present calc., with $q = 74\ \mu\mathrm{m}^{-1}$)		0.16	0.16

so the lh–hh transitions do not occur.

Then the generalisation of § 4.1 from two to three components is straightforward. The components are labelled with suffix i ($= 1, 2, 3$), and k_{Fi}, v_{Fi}, m_i, e_{Fi} are the Fermi wavevector, Fermi velocity, effective mass and Fermi energy of component i. The labelling is such that $v_{F3} \leqslant v_{F2} \leqslant v_{F1}$. The mass values are taken, for straightforward comparison, the same as those of PSW, namely $m_e = 0.68m_0$, $m_{LH} = 0.075m_0$, $m_{HH} = 0.62m_0$. Then components 1, 2, 3 are e, LH, HH respectively. Component 3 is taken to be the reference plasma for the purpose of defining the reduced variables

$$r_{ki} = k_{F3}/k_{Fi} \qquad r_{vi} = v_{F3}/v_{Fi} \qquad (i = 1, 2).$$

The reduced wavevector of the plasma wave is $z = q/2k_{F3}$, and the reduced phase velocity is $u = \omega/qv_{F3}$. The dielectric function is now

$$\varepsilon(z, u) = 1 + 2c_1 g(r_{k1}z, r_{v1}u) + 2c_2 g(r_{k2}z, r_{v2}u) + 2c_3 g(z, u)$$

since each pocket degeneracy ν_i ($i = 1, 2, 3$) is 1 in GaAs.

The general features to be expected from the solution of the condition for plasma modes, namely $\varepsilon = 0$, can be anticipated from the results of § 4. There it was found that an acoustic plasmon does not always exist, the system parameters for which it exists being shown in figure 8. In a three-component plasma a maximum of three plasma modes (which may be named ordinary plasmon, upper acoustic plasmon, lower acoustic plasmon) may be expected, with fewer than two acoustic modes existing in some cases. This expectation has been verified by numerical solutions in the present work.

Figure 15 shows qualitatively the relation between the real part u' of the reduced phase velocity of the three possible plasma branches and the six lines of discontinuity. (The value of u'' that enters is of course that of the plasma mode with which the line of discontinuity is currently being compared.)

We have solved the equation $\varepsilon = 0$ for the GaAs electron–hole plasma for several values of carrier density, including the two at which PSW claim observation of acoustic plasmons. The densities and other parameters are given in table 1. The value 12.9 was used for ε_{bg} (Hass and Henvis 1962), i.e. the relative permittivity at frequencies below the optical phonon frequency ($\simeq 30$ meV) of GaAs, because the acoustic plasmons turn out with frequencies well below 30 meV, even for the largest practical wavevectors and carrier densities.

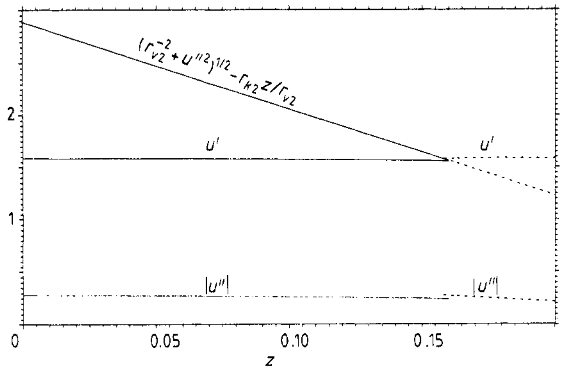

Figure 16. The real part (u') and magnitude of imaginary part ($|u''|$) of the reduced phase velocity of the acoustic plasmon versus reduced wavevector z in a GaAs electron–hole plasma with carrier density $n_e = 7 \times 10^{17}\,\text{cm}^{-3}$. Conversion of units: $q/\text{nm}^{-1} = 0.55z$, $\hbar\omega/\text{meV} = 18.6uz$.

In all of the GaAs electron–hole plasma systems that have been studied, there is no upper acoustic plasmon, but there is a lower acoustic plasmon, which will henceforth be referred to simply as the acoustic plasmon.

The acoustic plasmon spectrum for $n_e = 7 \times 10^{17}\,\text{cm}^{-3}$ is shown in figure 16. The first segment ends at $z = 0.1606$, when u' meets the indicated line of discontinuity. A second segment of the acoustic plasmon spectrum starts at $z = 0.1577$, i.e. there is a small overlap on the z axis, which is shown on an expanded scale in figure 17. In GaAs the discontinuity between segments 1 and 2 is almost certainly too small to be detected in the near future. The question whether the discontinuity (sometimes simply the end of the first segment with no further solutions) can be observed in other systems will be addressed in another paper.

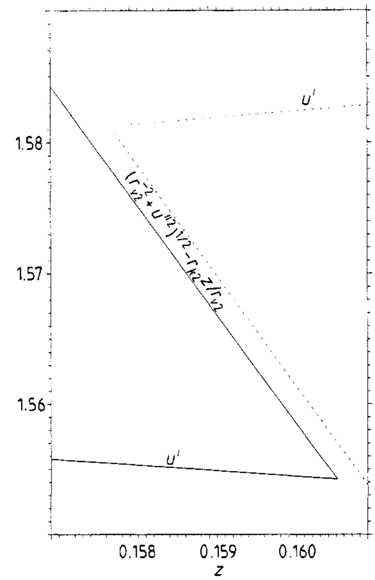

Figure 17. The overlap region of figure 16, shown on an expanded scale.

The numerical calculations give second segment solutions for z beyond the edge of figure 16, and up to $z = 0.5$. These larger z-values are, however, beyond the range of validity of the RPA. The generalisations to three components of the RPA conditions given in § 4.4.1 are

$$c_3 \nu_3^{1/3} \leqslant \tfrac{1}{3}(1 + R_1^{-1} r_{e1}^{-2} + R_2^{-1} r_{e2}^{-2})(1 + R_1^{-1} r_{e1}^{-1} + R_2^{-1} r_{e2}^{-1})^{-4/3} \tag{20}$$

where

$$\left.\begin{aligned} r_{ei} &= r_{ri} r_{vi} = e_{F3}/e_{Fi} \\ R_i &= \nu_3 r_{ki}^2/\nu_i r_{vi} \end{aligned}\right\} \qquad (i = 1, 2)$$

and

$$z \leqslant \min\{(c_3 \nu_3/6)^{1/2}, r_{k2}^{-1}(c_2 \nu_2/6)^{1/2}, r_{k1}^{-1}(c_1 \nu_1/6)^{1/2}\}.$$

(The pocket degeneracies ν_i are included in these formulae for generality, but are all equal to 1 in the GaAs electron–hole plasma.) Equality in equation (20) specialises, in the one-component case, to the usual RPA density condition $r_s^* \leqslant 1$. From experience with metals ($2 \leqslant r_s^* \leqslant 6$) it is concluded that the densities of the two GaAs electron–hole plasma systems considered (table 1) are sufficient for the RPA to be approximately valid.

The spectra for $n_e/10^{17}\,\text{cm}^{-3} = 3$ and 7 are almost the same (in reduced variables). At zero wavevector, the reduced phase velocity $u' + iu''$ is independent of density (with R_i and r_{vi} ($i = 1, 2$) constant). At $z = 0.15$ the change of $n_e/10^{17}\,\text{cm}^{-3}$ from 3 to 7 produces decreases of 0.7% in u' and 6% in $|u''|$, and an increase of 0.5% in z_c (the end of the first segment). This approximate independence of density, when the important ratios remain constant, is a general feature, exemplified by figure 12 in the two-component case.

It can be seen from figure 16 that the real part, u', of the phase velocity is nearly independent of z, up to the RPA limit. PSW found their evidence for an acoustic plasmon by back-scattering of 1.916 eV laser light. Using Aspnes and Studna's (1983) value of the GaAs refractive index at this frequency, namely 3.83, gives a wavevector $q = 74\,\mu\text{m}^{-1}$ for the created acoustic plasmon. (PSW quote $0.7 \times 10^6\,\text{cm}^{-1}$ as the scattering wavevector.) The calculated values of plasmon energy and damping for the two experimental systems for which PSW claim acoustic plasmons are given in table 1.

The main source of possible error in the calculations presented here is the fact that the wavevector $q = 74\,\mu\text{m}^{-1}$ is, for both densities, about equal to the maximum wavevector at which the RPA is expected to be valid. This error is not known, and might be as high as a few $\times 10\%$.

The calculations reported here give acoustic plasmon energies (and phase velocities) about 13% less than the calculations of PSW. PSW do not give separate numerical values for the measured energies, but say they are in agreement with the calculations. From the experimental trace given in figure 2(a) of PSW ($n_e = 7 \times 10^{17}\,\text{cm}^{-3}$) an error bar of about $\pm 10\%$ appears reasonable. In the case $n_e = 3 \times 10^{17}\,\text{cm}^{-3}$ the reality of a resonant response above the noise level (PSW figure 1(b)) is not established. Thus the calculations presented here are consistent with the limited experimental evidence available. The (Landau) damping of the acoustic plasmons has also been calculated (table 1) and found sufficiently small to permit detection.

There is, however, an important difference of principle between the present calculation and the calculation of PSW. The basis of PSW's calculation is a 'Pines–Froehlich' approximation

$$\omega/q = (\omega_{p3}^2 + \omega_{p2}^2)^{1/2}/\kappa_{TF1} \tag{21}$$

where ω_{pi} and κ_{TFi} are the usual plasma frequency and Thomas–Fermi wavevector parameters of component i. The use of (21) is, however, not self-consistent, because it is based on the assumption

$$(v_{F2} \text{ and } v_{F3}) \ll \omega/q \ll v_{F1}$$

yet its application to the GaAs electron–hole plasma leads to $\omega/q < v_{F2}$. For example, when $n_e = 3 \times 10^{17}\,\mathrm{cm}^{-3}$, $v_{F2} = 1.1 \times 10^5\,\mathrm{m\,s}^{-1}$ and $\omega/q = 8 \times 10^4\,\mathrm{m\,s}^{-1}$ is obtained. The correct conclusion from the finding '$\omega/q < v_{F2}$' is that the upper acoustic plasmon (which is what (21) is describing) probably does not exist. The numerical solution of the exact three-component RPA expression for ε shows that there is indeed no such solution. The resonant response observed by PSW can, however, be identified (tentatively) with the lower acoustic plasmon. A decisive demonstration of acoustic plasmons should measure ω at several q-values and also the density dependence of ω/q. For comparison with theory the exact solution of the RPA dielectric function will usually be needed, because of the severe conditions (17) for accuracy of the Pines–Froehlich approximation.

6. Discussion

Our model of a two-component semi-metal, which under some conditions sustains acoustic plasmons, has four parameters ($c_2\nu_2$, $c_1\nu_1$, r_v, R), which are summarised in § 4.5. The set of all possibilities is therefore potentially complicated. We find, however, that the general features of acoustic plasmons, within the range for which the RPA is valid, are not complicated. They depend principally on only two parameters, r_v and R, and these parameters determine exactly the properties of acoustic plasmons at zero wavevector.

For these reasons we have in this paper emphasised a general survey intended to be convenient for the consideration of the prospects for acoustic plasmons in a wide range of semi-metals and degenerate semiconductors.

The evidence for the existence of acoustic plasmons in homogeneous media is sparse. (Excitation analogous to acoustic plasmons have, however, been observed in multi-layered systems, for example in GaAs/$Al_xGa_{1-x}As$ by Olego *et al* (1982).) This sparsity may be considered surprising, since acoustic plasmons were predicted long ago. Ruvalds (1981) in his review titled 'Are there acoustic plasmons?' described them as elusive. He also mentioned a factor contributing to lack of success, which is that usually acoustic plasmons are not well coupled to several standard probes of condensed matter excitations, namely x-rays, neutrons, phonons and fast electrons. Raman spectroscopy, angle-resolved electron-energy-loss spectroscopy and inelastic electron-tunnelling spectroscopy (IETS) are, however, more suitable, in terms of energy and momentum transfer. In the last of these techniques, IETS, momentum resolution is not present in the basic form, but can be obtained if the semi-metal electrode of the tunnel diode is a thin parallel-sided size-quantised film (Jaklevic and Lambe 1975, Finkenrath and Stoeckel 1987, Cottey *et al* 1987).

There is one encouraging indication that acoustic plasmons exist. This was obtained (Pinczuk *et al* 1981) by Raman spectroscopy on a photo-excited electron–hole plasma in GaAs. We reanalysed these results in § 5, allowing for the three-component nature of the system. More experimental results, both in GaAs and in other substances, are needed before it can be said that acoustic plasmons (their absence in some materials as well as their presence in others) are fully understood and tested. We will present the results of calculations for other semi-metals and semiconductors in another paper.

A further reason for slow progress in detecting and testing the properties of acoustic plasmons in homogeneous media may be the restricted nature of the solution (18), especially if the further restrictions (19) are made, as they often have been. We see from our work that the range of parameters predicting moderate or small damping is greater than the range obtained from the special case (18). Neither the condition $r_v \ll 1$ (i.e. $v_{F2} \ll v_{F1}$), nor the condition $m_1^* \ll m_2^*$ is necessary, according to our theory. On the other hand, the strip of r_v–R space near the edge of the existence domain (figure 8) supports acoustic plasmons only for small wavevectors.

Acknowledgment

B Bennacer thanks the Algerian Ministry of Higher Education for a research grant.

References

Appel J and Overhauser A W 1982 *Phys. Rev.* B **26** 507–12
Aspnes D E and Studna A A 1983 *Phys. Rev.* B **27** 985–1009
Bennacer B 1987 *MPhil Thesis* University of East Anglia
Blank A Ya and Gulyaev Yu V 1984 *JETP Lett.* **39** 58–61
Chakraborty T 1984 *Phys. Rev.* B **29** 3975–81
Cottey A A 1985 *J. Phys. F: Met. Phys.* **15** L203–6
Cottey A A, Enders R, Finkenrath H, Stoeckel T and Uhle N 1987 *Thin Solid Films* **149** 149–61
Das Sarma S and Quinn J J 1982 *Phys. Rev.* B **25** 7603–18
Finkenrath H and Stoeckel T 1987 *Thin Solid Films* **149** 143–8
Froehlich H 1968 *J. Phys. C: Solid State Phys.* **1** 544–8
Ganguly B N and Wood R F 1972 *Phys. Rev. Lett.* **28** 681–4
Hass M and Henvis B W 1962 *J. Phys. Chem. Solids* **23** 1099–104
Heitmann D 1986 *Surf. Sci.* **170** 332–45
Jaklevic R C and Lambe J 1975 *Phys. Rev.* B **12** 4146–60
Klimontovich Yu L and Silin V P 1960 *Sov. Phys.–Usp.* **3** 83–114
—— 1961 *Plasma Physics* ed. J E Drummond (New York: McGraw-Hill) pp 35–87
Landau L D 1946 *J. Phys. USSR* **10** 25–34
Lindhard J 1954 *K. Danske Vidensk. Selsk., Mat.-Fys. Meddr.* **28** 1–57
Lomtev A I and Bol'shinskii L G 1985 *Sov. Tech. Phys. Lett.* **11** 348–9
Olego D, Pinczuk A, Gossard A C and Wiegmann W 1982 *Phys. Rev.* B **25** 7867–70
Oliva J and Ashcroft N W 1982 *Phys. Rev.* B **25** 223–36
—— 1984 *Phys. Rev.* B **29** 1067–8
Pashitskiĭ E A 1969 *Sov. Phys.–JETP* **28** 1267–71
Pinczuk A, Shah J and Wolff P A 1981 *Phys. Rev. Lett.* **47** 1487–90
Pines D 1956 *Can. J. Phys.* **34** 1379–94
—— 1963 *Elementary Excitations in Solids* (New York: Benjamin) pp 248–9
Platzman P M and Wolff P A 1973 *Waves and Interactions in Solid State Plasmas; Solid State Phys. Suppl.* **13** 1–304 (New York: Academic)

Rothward A 1972 *Phys. Rev.* B **2** 3560–71
Ruvalds J 1981 *Adv. Phys.* **30** 677–95
Schaefer F C and von Baltz R 1987 *Z. Phys.* B **69** 251–5
Silin V P 1952a *Zh. Eksp. Teor. Fiz.* **23** 641–8
—— 1952b *Zh. Eksp. Teor. Fiz.* **23** 649–59
—— 1955 *Trudy Fiz. Inst. P N Lebedeva* **6** 199–268
Singwi K S and Tosi M P 1981 *Solid State Phys.* **36** 177–266
Sinha S K and Varma C M 1983 *Phys. Rev.* B **28** 1663–6
Takada Y 1987 *J. Phys. Soc. Japan* **43** 1627–36
Vignale G and Singwi K S 1982 *Solid State Commun.* **44** 259–61
—— 1985 *Phys. Rev.* B **31** 245–50
Wooten F 1972 *Optical Properties of Solids* (New York: Academic) pp 193–4